

**INFLUENCE OF THE SOLVENT AND EXCITED STATE  
PROTOTROPIC EQUILIBRIA ON PHOTOCHEMICAL  
INTRAMOLECULAR ACYLATION OF *trans*-3-(2-HYDROXY-  
BENZYLIDENE)-4,5-DIHYDROFURAN-2(3*H*)-ONE**

BRUNO MARCANDALLI, ELENA SELLI, IGNAZIO RENATO BELLOBONÒ and  
LUCA BASINI

*Cattedra di Chimica, Dipartimento di Chimica Fisica ed Elettrochimica, University of  
Milan, I-20133 Milano (Italy)*

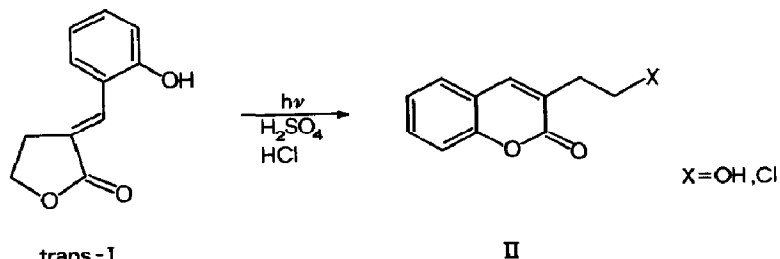
(Received March 19, 1986; in revised form July 7, 1986)

### Summary

The solvent dependence of the kinetics of the geometrical isomerization of *trans*-3-(2-hydroxybenzylidene)-4,5-dihydrofuran-2(3*H*)-one and the subsequent intramolecular acylation of the *cis* substrate was studied. Even if the quantum yields  $\Phi_1$  and  $\Phi_2$  of the two processes increase on increasing the polarity of the methanol solutions, addition of water is found to quench dramatically  $\Phi_1$  and  $\Phi_2$ . This behaviour is interpreted in terms of the proton exchange equilibria of the excited singlet state. A detailed analysis of the dependence of the fluorescence on the pH was carried out and a mechanistic model which is able to describe satisfactorily the experimental results is proposed.

### 1. Introduction

The formation of coumarins from 3-(2-hydroxybenzylidene)-furan-2(3*H*)-ones has been studied previously by a number of researchers both outside [1 - 5] and within [6 - 8] our laboratory under various experimental conditions. It has been shown that the reaction of *trans*-3-(2-hydroxybenzylidene)-4,5-dihydrofuran-2(3*H*)-one (*trans*-I) to give II (see Scheme I) is quantitative whether it is performed by acid catalysis or by photochemical methods.



trans - I  
Scheme I.

For acidic media a mechanism has been proposed which involves rapid *trans*-*cis* isomerization of *trans*-I followed by nucleophilic attack of the phenolic hydroxy group on the carbon atom of the carbonyl [6].

In the photochemical reaction, two steps characterized by markedly different quantum yields  $\Phi_1$  and  $\Phi_2$  can be easily distinguished. The first consists in the geometrical isomerization of *trans*-I; it does not undergo concentration quenching and is likely to occur directly through a singlet  $^1(\pi, \pi^*)$  excited state in which the plane of the aromatic ring is perpendicular to the furan system. The second step is strongly influenced by the concentration of the substrate and can be tentatively attributed to a planar  $^3(n, \pi^*)$  state. In both steps the quantum yield shows a marked wavelength dependence, suggesting the presence of barriers to internal conversion.

Some preliminary experiments during our previous research [7] showed drastic and unexpected quenching of both  $\Phi_1$  and  $\Phi_2$  by water. This fact, together with our interest in excited state equilibria, led us to investigate in detail the effect of the solvent, and in particular of water, on the fluorescence properties of *trans*-I and on the kinetics of the reaction shown in Scheme I.

In this paper, we report the results of this study and discuss in detail the acid-base properties of the singlet excited state of *trans*-I and the mechanism of action of water on the aforementioned reaction.

## 2. Experimental details

### 2.1. Materials

*trans*-I was synthesized and purified as described previously [6]. Spectrograde solvents purchased from Fluka AG (Switzerland) were used in all the experiments.

### 2.2. Methods

Absorption measurements were performed with a Perkin-Elmer model 552 S spectrophotometer. Fluorescence spectra were obtained using a Perkin-Elmer model 650-10 S spectrofluorometer. A thermostatic water bath circulator (MLW 16, G.D.R.) was employed to control the solution temperature at  $25.00 \pm 0.05$  °C. The pH was measured by means of an Amel (Italy) pHmeter with a combined electrode.

Absorption, fluorescence and kinetic experiments were all performed on solutions approximately  $5 \times 10^{-5}$  M in *trans*-I.

The absorption spectra of *trans*-I, *cis*-I and II ( $X \equiv OH$ ) are shown in Fig. 1.

The pH (or  $H_0$ ) values of the samples were adjusted with  $HClO_4$  (or  $H_2SO_4$  for very low  $H_0$ ) and NaOH. The use of buffer solutions was avoided because high concentrations of buffer ions may complicate the treatment of fluorometric titration data [9]. In fluorescence measurements excitation was always effected at the isosbestic point of the acid-base equilibrium of *trans*-I

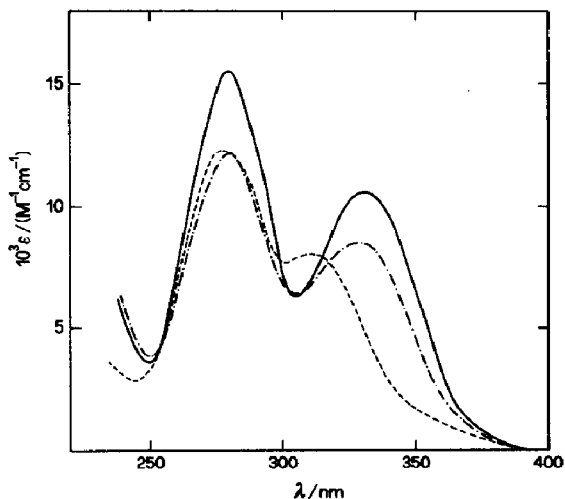


Fig. 1. Molar extinction coefficients  $\epsilon$  of *trans*-I (—), *cis*-I (- · -) and II (- - -) in methanol.

( $\lambda_{\text{exc}} = 345 \text{ nm}$ ). Nitrogen purging of the solutions did not affect any of the results.

The quantum yields  $\Phi_1$  and  $\Phi_2$  were determined under irradiation at 366 nm with home-made apparatus. The light source was a 700 W high pressure mercury lamp (Italquartz, Italy) and a monochromatic light beam was obtained by means of an Oriel interference filter. A system of quartz lenses and slits was used to collimate the radiation beam impinging on the sample cell. At the wavelength employed the absorption of the solution was always very small ( $A < 0.1$ ), so that homogeneous irradiation of the sample could be assumed. Potassium ferrioxalate was used for the actinometry, according to the method of Hatchard and Parker [10]. The kinetics of the reaction were followed spectrophotometrically. As we knew the spectra of pure *trans*-I, *cis*-I and II (Fig. 1) [6] we were able to determine the time variations of the concentrations of all the species present in solution, using a least-squares method (in matrix form) based on absorbance data at ten evenly spaced wavelengths [11]. The numerical evaluation of  $\Phi_1$  and  $\Phi_2$  was carried out by employing the Niemann-Mausser method of formal integration [12, 13], adapted to a simple mechanism consisting of two consecutive steps. However, simply adopting the spectrophotometric extinction coefficients  $\epsilon(\lambda)$  in the calculation of the fraction of light absorbed by the system under investigation can lead to systematic errors in the evaluation of quantum yields because of the large bandwidth of the filter. In order to avoid these artefacts, instead of  $\epsilon(\lambda)$  the quantities

$$\bar{\epsilon} = \frac{\int \epsilon(\lambda) T(\lambda) d\lambda}{\int T(\lambda) d\lambda}$$

were used, where  $T(\lambda)$  is the transmission characteristic of the filter, and the integral has been numerically calculated over the entire wavelength range of

the radiation transmitted by the filter. It may be easily shown that in the case of a large bandwidth, if absorbancies are small, the Beer-Lambert law still holds if  $\bar{\epsilon}$  is used instead of  $\epsilon(\lambda)$ .

All the calculations were executed on an Apple McIntosh computer.

### 3. Results and discussion

#### 3.1. Solvent effect on the absorption and emission spectra of *trans*-3-(2-hydroxybenzylidene)-4,5-dihydrofuran-2(3H)-one

The first step in our investigation was to study the effect of the solvent on the absorption and fluorescence spectra of *trans*-I in order to obtain information on the polarity and the geometry of its ground and excited states as well as on the presence and the nature of specific interactions with the medium.

Absorption and emission spectra of *trans*-I were recorded in various solvents; the corresponding  $\tilde{\nu}_{\max}(\text{abs})$  and  $\tilde{\nu}_{\max}(\text{flu})$  are listed in Table 1, together with the dielectric constants  $\epsilon$  and the refractive indices  $n$  of the solvents.

The absorption band at about 330 nm is blue shifted in hydrogen-bonded solvents, while the transition at about 280 nm is hardly affected by the solvent. The bathochromic shift of both bands in comparison with enones [14] indicates extensive conjugation of the furanone system with the aromatic ring.

When compared with the values in cyclohexane, fluorescence maxima are always red shifted in polar and protic solvents. In pure water, the bands at 455 nm and 520 nm split in two; in no other solvent was this observed. In

TABLE 1

Absorption and fluorescence maxima  $\tilde{\nu}_{\max}(\text{abs})$  and  $\tilde{\nu}_{\max}(\text{flu})$  of *trans*-3-(2-hydroxybenzylidene)-4,5-dihydrofuran-2(3H)-one in different solvents

Solvent	Dielectric constant $\epsilon$	Refractive index $n$	$\tilde{\nu}_{\max}(\text{abs})$ (cm <sup>-1</sup> )	$\tilde{\nu}_{\max}(\text{flu})$ (cm <sup>-1</sup> )
Cyclohexane	2.02	1.4262	30120 - 35840	25525
1,1,2-Trichloroethylene	4.22	1.5074	30490	25445
Diethyl ether	4.34	1.3524	31055 - 36630	26315
Ethyl acetate	6.02	1.3724	31150 - 36630	25950
Acetic acid	6.15	1.3719	31150 - 36630	24096
1,1,1-Trichloroethane	7.53	1.4379	30770 - 36100	25510
1,1,2,2-Tetrachloroethane	8.08	1.49165	30675 - 35840	25000
1-Butanol	17.51	1.3993	30210 - 35840	24390
2-Propanol	19.92	1.3772	30395 - 35970	24210
Ethanol	24.55	1.3614	30395 - 35970	23810
Diethylene glycol	31.69	1.4475	30210 - 35840	23040
Methanol	32.70	1.3284	30580 - 36100	23364
Water	78.39	1.3330	31055 - 35970	21740 - 19230

order to discriminate between polarity effects and specific interactions, an analysis in terms of the Bilot-Kawski equation was carried out [15]. In this approach it is assumed that the rotational relaxation time of the solvent molecule is much shorter than the lifetime of the excited state, neglecting all terms depending on polarizability changes, and it was recently found [16] to afford results that were better than all the other existing theories.

The Bilot-Kawski equation is

$$\begin{aligned} \tilde{\nu}(\text{abs}) - \tilde{\nu}(\text{flu}) &= \frac{(\mu_e - \mu_g)^2}{hca^3} \\ &\times \frac{\{(\epsilon - 1)/(2\epsilon + 1)\} - \{(n^2 - 1)/(2n^2 + 2)\}}{\{1 - \beta(n^2 - 1)/(2n^2 + 2)\}^2 \{1 - \beta(\epsilon - 1)/(2\epsilon + 2)\}} \\ &+ \text{constant} \\ &= \frac{(\mu_e - \mu_g)^2}{hca^3} \gamma + \text{constant} \end{aligned} \quad (1)$$

where  $\tilde{\nu}(\text{abs})$  and  $\tilde{\nu}(\text{flu})$  are the wavenumbers of the absorption and fluorescence band maxima,  $h$  is Planck's constant,  $\epsilon$  is the solvent dielectric constant,  $n$  is the solvent refractive index,  $c$  is the speed of light,  $\beta$  is a factor approximately equal to unity,  $\mu_e$  and  $\mu_g$  are the dipole moments of the excited and ground states respectively and  $a$  is the Onsager cavity radius.

Therefore a plot of  $\tilde{\nu}(\text{abs}) - \tilde{\nu}(\text{flu})$  vs.  $\gamma$  (the polarizability function of eqn. (1)) should give a straight line and, if  $a$  is known,  $(\mu_e - \mu_g)$  can be evaluated from the slope. The plot obtained is shown in Fig. 2, in which the full line corresponds only to solvents which cannot form hydrogen bonds with the substrate. With this limitation a reasonably good correlation is ob-

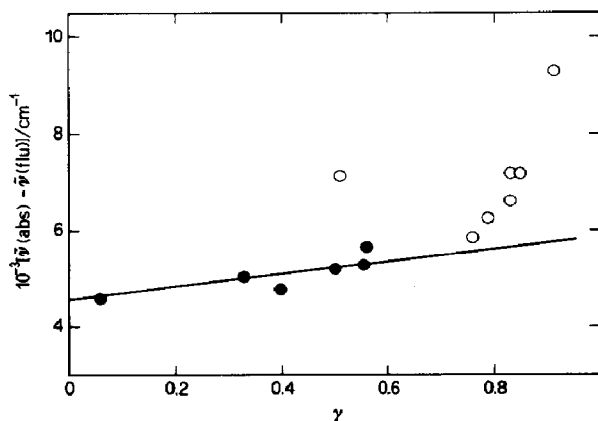


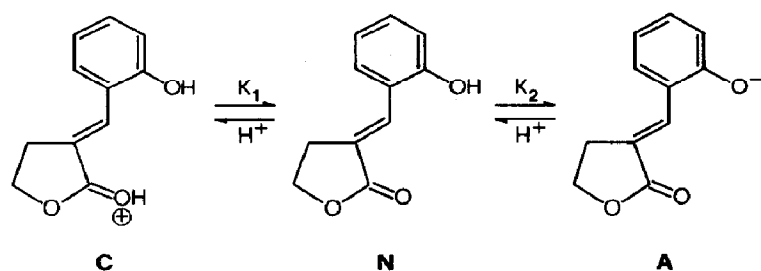
Fig. 2. Stokes shift ( $\tilde{\nu}(\text{abs}) - \tilde{\nu}(\text{flu})$ ) of *trans*-I as a function of the polarity parameter  $\gamma$  of Bilot and Kawski (see eqn. (1)). The open circles refer to alcoholic solvents (excluded from the regression analysis).

tained ( $r = 0.99$ ) and, if  $a$  is taken to be  $5 \text{ \AA}$ , the slope of the straight line yields a value of 5.7 debyes for  $(\mu_e - \mu_g)$ .

Even if this value is very approximate, it clearly indicates that the  $S_1$  state is rather polar and has considerable charge transfer character. This is further confirmed by the action of alcoholic solvents and water. In this case, the large increase in the Stokes shift of *trans*-I can be interpreted as an enhancement of charge transfer resulting from the combined hydrogen-bond donor and acceptor properties of the amphiphilic solvents. Hydrogen bonding to the hydroxyl group favours conjugation of the lone pairs of the hydroxyl oxygen with the aromatic system, while hydrogen bonding to the carbonyl oxygen increases the electron density of the carbonyl group. This process is promoted by the hydrogen donor and acceptor properties of the solvent until, in water, deprotonation of the hydroxyl group in the  $S_1$  state occurs and the excited state anion appears ( $\lambda_{\text{max}} = 528 \text{ nm}$ ); this is discussed in detail in Section 3.2.

### 3.2. Ground and excited state prototropic equilibria of *trans*-I

In the electronic ground state of *trans*-I in aqueous solution three molecular species are spectroscopically detectable in the acidity range spanning from pH 12 to  $H_0 - 11$ . The corresponding acid-base equilibria are given in Scheme II.



Scheme II.

At  $\text{pH} > 12$  the substrate undergoes an irreversible moderately fast degradation which is probably due to the hydrolysis of the lactone moiety.

The absorption maxima in water of the anionic form (A) are 386 and 248 nm, and those of the neutral form (N) are 325 and 279 nm.

The protonated species (C) cannot be obtained in pure form even in concentrated  $\text{H}_2\text{SO}_4$ ; 340 and 300 nm can be given as approximate estimates of the wavelengths of the maxima.

$\text{p}K_1$  and  $\text{p}K_2$  were evaluated from absorption spectroscopy measurements and were found to be  $-10$  and  $8.99 \pm 0.05$  respectively.

In the fluorescence spectra, at  $\text{pH} > 11$  the only absorbing and emitting species is the anion, with an emission peak at 528 nm.

Between  $\text{pH} 8$  and  $\text{pH} 1$ , where ground state *trans*-I is present only in its neutral form N, the fluorescence spectrum consists of two bands of com-

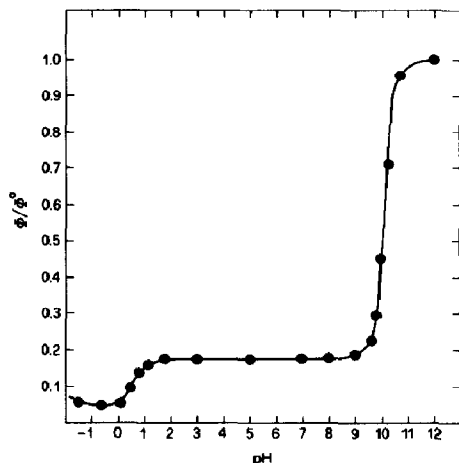


Fig. 3. Variation in the relative fluorescence efficiencies of *trans*-I as a function of pH.

parable and practically invariant intensities. The maximum wavelengths are 520 and 455 nm.

As the acidity increases, in the region from pH 1 to  $H_0 - 2$ , the fluorescence is markedly quenched and the band at 520 nm almost completely disappears.

For  $H_0 < 2.0$ , the fluorescence spectra undergo major changes; these are not discussed in this paper, as they will be the subject of a future paper devoted to the effect of acidity on the photochemical intramolecular acylation of *trans*-I.

A more quantitative picture may be obtained by inspection of Fig. 3, in which the pH dependences of the fluorescence quantum efficiencies are shown.

The band at 528 nm in the basic region can reasonably be considered to originate from the excited anion ( $A^*$ ) and that at 455 nm may be reasonably attributed to the excited neutral form ( $N^*$ ). In fact, by plotting the emission  $\tilde{\nu}_{\max}(\text{flu})$  in various protic solvents, in which only the neutral form is present, against the empirical solvent polarity parameter  $\pi^*$  [17], the wavelength of the  $N^*$  peak can be obtained to a good approximation by extrapolation to the value of  $\pi^*$  for water.

A more quantitative analysis of the fluorometric titration data provides further confirmation of the assignments proposed above. An estimate of the excited state equilibrium constant  $K_2^*$  of the reaction



can be obtained by application of the Förster cycle to the spectral data and the value of the ground state  $pK_2$  determined spectrophotometrically.

According to this method, which neglects the entropy differences of protolytic dissociation in the ground and excited states, the  $pK$  of the corresponding equilibria of the two energy levels are related by the equation

$$pK - pK^* = 2.1 \times 10^{-3}(\tilde{\nu}_a - \tilde{\nu}_b) \quad (3)$$

where  $\tilde{\nu}_a$  and  $\tilde{\nu}_b$  are the wavenumbers (in reciprocal centimetres) of the  $0 \rightarrow 0$  transition of the acid and base respectively [18]. The mean frequencies of the absorption and fluorescence maxima were assumed to be those of the pure electronic transition and a  $pK_2^*$  value of 0.69 was calculated.

Even considering the approximations of the method itself, this result shows conclusively that the hydroxyl group is much more acidic in the singlet excited state than in the ground state. This was not unexpected, as this is behaviour typical of the phenolic OH group.

The fluorometric titration curves depicted in Fig. 3 show more complex behaviour than the corresponding absorption data, but it should be remembered that the variations in the relative fluorescence quantum yields of acids and bases with pH are governed by the kinetics and the mechanisms of the prototropic reactions in the excited states [9].

If we consider the region from pH 12 to pH 0, our data show two inflection points, one at pH 10 and the other at about pH 0.7; in the mid-pH region, the relative fluorescence quantum yield  $\Phi/\Phi^\circ$ , *i.e.* the ratio between the quantum yields at different pHs to that of the pure anionic form, is practically independent of pH, with a value of  $0.15 \pm 0.06$ . In the absence of buffer ions, as in our experiments, the procedure of Weller [19, 20] and simple steady state kinetics give the relative emission efficiencies for reaction (2) as

$$\frac{\Phi}{\Phi^\circ} = \frac{k_p \tau_N}{1 + k_p \tau_N + k_{-p} \tau_A [H^+]} \quad (4)$$

where  $\tau_N$  is the lifetime of  $N^*$  in the lowest excited singlet state in the absence of excited state proton transfer.

This model can be easily applied to our experimental curves, if we consider the rates of fluorescence decay and excited state proton exchange to be comparable. Therefore the inflection at pH 10 corresponds to the ground state  $pK_2$  while that at pH 0.7 corresponds to  $pK_2^*$ . The latter value is in excellent agreement with the  $pK_2^*$  evaluated from the Förster cycle. At pHs around neutrality, where  $k_{-p} \tau_A [H^+]$  is small in comparison with  $k_p \tau_N$ , eqn. (4) can be simplified to

$$\frac{\Phi}{\Phi^\circ} = \frac{k_p \tau_N}{1 + k_p \tau_N} = \text{constant} \quad (5)$$

which corresponds to the plateau in the  $(\Phi/\Phi^\circ)$  vs. pH plot and, from our experimental data, gives  $k_p \tau_N = 0.18$ .

The discrepancy between  $pK_2$  measured by absorption spectroscopy and that measured by spectrofluorometry is probably due to the fluorescence band undergoing a solvent shift at high basicities.



TABLE 2

Quantum yields of photochemical *trans*-*cis* isomerization of *trans*-3-(2-hydroxybenzylidene)-4,5-dihydrofuran-2(3*H*)-one ( $\Phi_1$ ) and of intramolecular acylation of *cis*-3-(2-hydroxybenzylidene)-4,5-dihydrofuran-2(3*H*)-one ( $\Phi_2$ ) in various solvents

Solvent	$\Phi_1$	$\Phi_2$
<i>n</i> -Hexane	0.22	0.12
1-Butanol	0.37	0.16
Ethanol	0.63	0.17
Methanol	0.64	0.18
5wt.%methanol-95wt.%water	0.36	0.073
10wt.%methanol-90wt.%water	0.30	0.048
12wt.%methanol-88wt.%water	0.27	0.040
15wt.%methanol-85wt.%water	0.23	0.032
20wt.%methanol-80wt.%water	0.20	0.028

### 3.3. Effect of the solvent on intramolecular acylation of *trans*-I

The quantum yields of geometrical isomerization of *trans*-I ( $\Phi_1$ ) and of intramolecular acylation of *cis*-I ( $\Phi_2$ ) in various solvents and in water-methanol mixtures are reported in Table 2. If we take only anhydrous solvents into consideration, a general increase in both  $\Phi_1$  and  $\Phi_2$  but especially in  $\Phi_1$  is observed with increasing solvent polarity. Plotting  $\ln \Phi_i$  against the empirical solvent polarity parameter  $E_T$  [21] results in acceptably linear correlations; the corresponding correlation coefficients  $r$  are 0.92 and 0.99 for  $\Phi_1$  and  $\Phi_2$  respectively.

As discussed in ref. 7, the photochemical *trans*-*cis* isomerization of *trans*-I occurs through a singlet  $\pi, \pi^*$  excited state with the aromatic ring plane perpendicular to the furan system; this state is highly polar and, as a consequence, it should be strongly stabilized by polar solvents, facilitating the rotation process. However, the much lower polarity of the planar  $^3(n, \pi^*)$  state responsible for the acylation step leads to the influence of the solvent on  $\Phi_2$  being much smaller than on  $\Phi_1$ .

Further confirmation of the singlet nature of the excited state involved in the isomerization reaction is the linear correlation ( $r = 0.96$ ) of  $\ln \Phi_1$  with  $\tilde{\nu}_{\max}(\text{flu})$ , the fluorescence maximum wavenumber of *trans*-I, indicating that the factors involved in the stabilization of the first singlet excited state also play an important role in the photochemical isomerization process.

Water, even in small quantities, quenches drastically the quantum yields of both processes, so that in 40wt.%methanol-60wt.%water II is not produced and only *cis*-I is formed with a very low quantum yield. This has been exploited for the preparation of pure *cis*-I [7].

Processes occur in water which are missing in other solvents, and these compete with the two reactions that we have considered. These additional processes are clearly responsible for the change in behaviour. The complex acid-base equilibria of the singlet excited state in water certainly modify the mechanism of the photoisomerization step.

In fact, as soon as small amounts of water are added to a methanol solution of *trans*-I, in the absence of buffer, a fluorescence band appears at 520 nm corresponding to the emission of the anion. The intensity of this band increases steadily with increasing water content.

If we assume that the excited anion does not contribute significantly to the formation of *cis*-I, because of the higher electron density of the isomerizable double bond, the following mechanistic scheme can be proposed.

<i>Reaction</i>	<i>Rate</i>
$trans\text{-I} \xrightarrow{h\nu} N^*$	$I_a$
$N^* \longrightarrow trans\text{-I}$	$k_t[N^*]$
$N^* \longrightarrow trans\text{-I}$	$k_f[N^*]$
$N^* \longrightarrow cis\text{-I}$	$k_r[N^*]$
$N^* + H_2O \longrightarrow A^* + H_3O^+$	$k_{-p}[N^*][H_2O]$
$A^* + H_3O^+ \longrightarrow N^* + H_2O$	$k_p[A^*][H_3O^+]$
$A^* \longrightarrow trans\text{-I}$	$k_t'[A^*]$
$A^* \longrightarrow trans\text{-I}$	$k_f'[A^*]$

$I_a$  is the absorbed radiation,  $N^*$  and  $A^*$  are the neutral and anionic forms of the singlet excited state of *trans*-I,  $k_t$  and  $k_f$  are thermal and radiative deactivation rate constants of  $N^*$ , while the corresponding primed terms refer to  $A^*$ ,  $k_p$  and  $k_{-p}$  which are defined in reaction (2), and  $k_r$  is the rate constant for isomerization from  $N^*$ .

Under conditions of steady state excitation, the rates of disappearance of  $N^*$  and  $A^*$  from the lowest excited singlet state are given by

$$-\frac{d[N^*]}{dt} = -I_a - k_p[A^*][H_3O^+] + [N^*](k_t + k_f + k_r + k_{-p}[H_2O])$$

$$= 0 \tag{6}$$

$$-\frac{d[A^*]}{dt} = [A^*](k_t' + k_f' + k_p[H_3O^+]) - k_{-p}[N^*][H_2O]$$

$$= 0 \tag{7}$$

$[N^*]$  and  $[A^*]$  can be determined from eqns. (6) and (7), and introduction of these values into the expression giving the rate of formation of *cis*-I

$$\frac{d[\text{cis-I}]}{dt} = k_r[\text{N}^*] \quad (8)$$

leads to

$$\Phi_1 = \frac{k_r(\tau_A^{-1} + k_p[\text{H}_3\text{O}^+])}{\tau_N^{-1}(\tau_A^{-1} + k_p[\text{H}_3\text{O}^+]) + \tau_A^{-1}k_{-p}[\text{H}_2\text{O}]} \quad (9)$$

where  $\tau_N = 1/(k_t + k_t' + k_r)$  and  $\tau_A = 1/(k_t' + k_t')$ .

In the absence of water,  $\text{A}^*$  is not formed appreciably and

$$\Phi_1^\circ = \tau_N k_r \quad (10)$$

Therefore from eqns. (9) and (10) one obtains

$$\frac{\Phi_1^\circ}{\Phi_1} = 1 + \frac{\tau_N k_{-p}[\text{H}_2\text{O}]}{1 + \tau_A k_p[\text{H}_3\text{O}^+]} \quad (11)$$

Under neutral conditions, as in our experiments,  $[\text{H}_3\text{O}^+] \sim 10^{-7} \text{ M}$  and, consequently,  $\tau_A k_p[\text{H}_3\text{O}^+] \ll 1$  if it is assumed that  $k_p$  is a diffusion-controlled reaction rate constant. In conclusion, eqn. (11) reduces to

$$\frac{\Phi_1^\circ}{\Phi_1} = 1 + \tau_N k_{-p}[\text{H}_2\text{O}] \quad (12)$$

Equation (12) gives a linear correlation between  $\Phi_1^\circ/\Phi_1$  and  $[\text{H}_2\text{O}]$ . The plot of the experimental data in Fig. 4 shows that our measurements are in good agreement ( $r = 0.992$ ) with eqn. (12) even if the model is based on the assumption that  $\tau_N$ ,  $\tau_A$ ,  $k_p$  and  $k_{-p}$  are independent of the solvent, which is certainly not completely correct.

Moreover,  $\tau_N k_{-p} = 0.23$  is obtained from the slope of the straight line in Fig. 4, which combined with  $\tau_N k_p = 0.18$  (from eqn. (5) in Section 3.2) gives

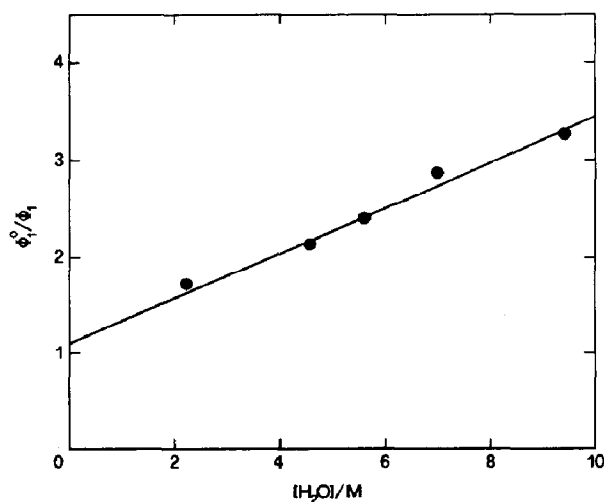


Fig. 4. Plot of the ratio of the quantum yields of the geometrical isomerization of *trans*-I in water-methanol mixtures ( $\Phi_1$ ) and in anhydrous methanol ( $\Phi_1^\circ$ ) vs. water concentration.

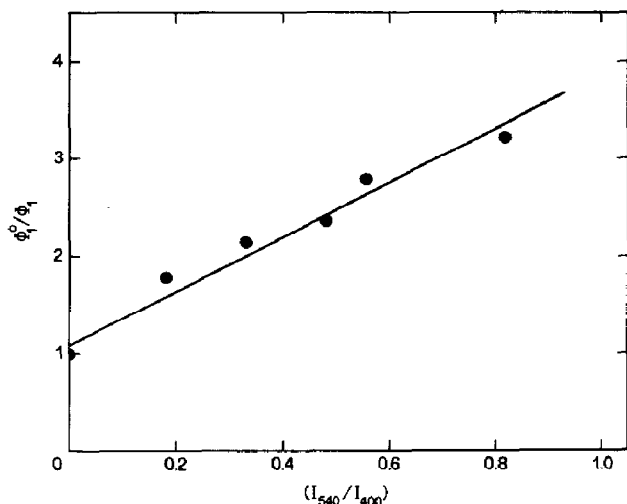


Fig. 5. Correlation of the ratio of the quantum yields of geometrical isomerization of *trans*-I in water-methanol mixtures ( $\Phi_1$ ) and in anhydrous methanol ( $\Phi_1^0$ ) with the ratio of fluorescence intensities at 540 nm and 400 nm ( $I_{540}/I_{400}$ ).

$K_2^* = 0.78$ ; this is in substantial agreement with the experimental  $K_2^*$  (0.16) if we take into account the differences due to solvent effects.

From eqns. (6) and (7)

$$\frac{[A^*]}{[N^*]} = \frac{k_{-p}[H_2O]}{\tau_A^{-1} + k_p[H_3O^+]} \quad (13)$$

which when inserted into eqn. (11) leads to

$$\frac{\Phi_1^0}{\Phi_1} = 1 + \frac{\tau_N}{\tau_A} \frac{[A^*]}{[N^*]} \quad (14)$$

An estimate of the ratio of the concentrations of the anionic and neutral excited forms is given by the ratio of the fluorescence intensities at two wavelengths of emission of the two molecular species which are sufficiently far apart that the overlap between the two bands is likely to be small. The linearity ( $r = 0.985$ ) of the experimental plot of  $\Phi_1^0/\Phi_1$  in different water-methanol solutions as a function of the ratios of the emission intensities at 540 nm and 400 nm (see Fig. 5) gives further support to our model.

Considering the effect of water on the acylation step, which was suggested to occur through a planar triplet state, even without performing direct phosphorescence measurements we can reasonably expect that the triplet  $pK^*$  will differ from the ground state values much less than the singlet  $pK^*$  [18]. However, the fluorescence spectra of *cis*-I show acid-base behaviour parallel to that of *trans*-I, with an emission peak corresponding to the anion at about 510 nm. Therefore it is probable that in this case increased competition with anion fluorescence and thermal deactivation results in the efficiency of the intersystem crossing and consequently the acylation quantum yield both being quenched.

## References

- 1 J. Thiele, R. Tischbein and E. Lossow, *Annalen*, 319 (1901) 180.
- 2 D. H. Marrian and P. B. Russel, *J. Chem. Soc.*, (1940) 753.
- 3 D. H. Marrian, P. B. Russel and A. R. Todd, *Biochem. J.*, 45 (1949) 533.
- 4 H. Zimmer, F. Haupter, J. Rothe, W. E. J. Schrof and R. Walter, *Z. Naturforsch.*, 184 (1963) 165.
- 5 H. Zimmer, F. Haupter, S. P. Kharidia, H. Pauling, R. G. Gailey, T. Pampalone, T. C. Purcell and R. Walter, *Tetrahedron Lett.*, (1968) 5435.
- 6 I. R. Bellobono, B. Marcandalli, L. Zanderighi and C. Parini, *J. Chem. Soc., Perkin Trans. II*, (1975) 1525.
- 7 I. R. Bellobono, L. Zanderighi, S. Omarini, B. Marcandalli and C. Parini, *J. Chem. Soc., Perkin Trans. II*, (1975) 1529.
- 8 I. R. Bellobono, E. Dubini Paglia, B. Marcandalli and M. Turi Cataldi, *Gazz. Chim. Ital.*, 109 (1979) 697.
- 9 S. G. Schulman, *Fluorescence and Phosphorescence Spectroscopy: Physicochemical Principles and Practice*, Pergamon, Oxford, 1977, p. 80.
- 10 C. G. Hatchard and C. A. Parker, *Proc. R. Soc. London, Ser. A*, 235 (1956) 518.
- 11 J. C. Sternberg, H. S. Stillo and R. H. Wendeman, *Anal. Chem.*, 32 (1960) 84.
- 12 H. J. Niemann and H. Mauser, *Z. Phys. Chem., N. F.*, 82 (1972) 295.
- 13 H. Mauser, D. J. Francis and H. J. Niemann, *Z. Phys. Chem., N. F.*, 82 (1972) 318.
- 14 J. A. Barltrop and J. D. Coyle, *Excited States in Organic Chemistry*, Wiley, Chichester, 1978, p. 176.
- 15 L. Bilot and A. Kawski, *Z. Naturforsch.*, 179 (1962) 621.
- 16 B. Koutek, *Collect. Czech. Chem. Commun.*, 43 (1978) 2368.
- 17 M. J. Kamlet and R. W. Taft, *J. Am. Chem. Soc.*, 98 (1976) 377.
- 18 I. Yu. Martinov, A. B. Demyashkevich, B. M. Uzhinov and M. G. Kuzmin, *Russ. Chem. Rev.*, 46 (1977) 1.
- 19 A. Weller, *Z. Elektrochem.*, 56 (1952) 662.
- 20 A. Weller, *Prog. React. Kinet.*, 1 (1961) 187.
- 21 C. Reichardt, *Solvent Effects in Organic Chemistry*, Verlag Chemie, Weinheim, 1979, p. 241.